NEUTRAL COMPRESSION IN THE W7-AS STELLARATOR DIVERTOR

K.McCormick, P.Grigull, H.Ehmler, F.Feng, G.Haas, J.P.Knauer and the W7-AS Team
Max-Planck-Institut für Plasmaphysik, , EURATOM, 85748 Garching, Germany

1. Introduction: The W7-AS stellarator (R=2m, a~0.12m for ι_a~5/9) has now been equipped with 10 discrete divertor modules (5 up, 5 down), allowing the concept of a boundary-island divertor to be experimentally evaluated for the first time in preparation for implementation on W7-X. Ideally, the divertor layout should foster neutral compression such that suitable pressures are attained in the subdivertor region for effective pumping (to enhance particle control) and in the main chamber to reduce charge-exchange sputtering and possibly promote high-confinement regimes. Intensive divertor experiments were initiated in March 2001. This paper reports on neutral pressure measurements in the subdivertor regions near where Ti getter-pumping is foreseen and in the main chamber. Relationships among parameters directly connected with neutral pressure (line-averaged density $\bar{n}_e$, upstream separatrix density n_{es}, heating power, ion flux to the target plates I_{sat}) are documented and placed in context with previous experience gained using inner-sector limiters instead of divertors.

Four ASDEX-type gauges are placed in subdivertors (3 upper divertors, 1 in a lower divertor) and five in the main chamber. Toroidal asymmetries are not prominent, so results (P_{up}, P_{down}) from only the up-down subdivertor pair are reported. The divertors are not toroidally continuous, thus one main-chamber gauge is placed near the bottom of the torus at the end of the lower divertor (P_{end}) and another sits near the inside wall below the midplane and above the inner lip of the lower divertor trough (P_{side}). The gauges were calibrated over 0.1-2x10^{-3} mbar. Actually, they are sensitive to the local gas flux, but due to baffling the neutrals are essentially at room temperature in the detector head. Hence, the values quoted are room-temperature-equivalent neutral pressures for within the main chamber.

2. Experiments: A ι_a~5/9 plasma configuration was studied, with the control coils activated such that the nearest target-plate to x-point distance was ~4cm, with upstream-downstream connection lengths along field lines of ~100m /1/. Two operational scenarios have emerged: a) "Normal Confinement" with core-edge interrelationships typical of the past and a new regime b) "Improved High-Density Confinement" (IHDC).

2.1 Normal Confinement: The principle discharge series involves three heating powers, P_{ecrh} = 0.3, 0.6 and 0.9MW with four density plateaus each, all in quasi steady-state. (These discharges were also used for a systematic study of carbon concentration vs. sources /2/.) Fig. 1a shows that n_{es} increases non-linearly with P_{ecrh} and with $\bar{n}_e$ in the fashion $n_{es} \sim \bar{n}_e^{0.34\text{-}0.56}$ over the range investigated, i.e. the global density profiles exhibit "peaking" with higher $\bar{n}_e$ or a "broadening" with higher P_{heat} phenomena already seen with the inner limiters /3,4/. Fig. 1b illustrates that the ion flux to the lower target plate (represented by the current to a single flush-mounted Langmuir at the peak of the strike zone) and P_{down} (also P_{up}) behave similarly as a function of n_{es}. Strikingly, both exhibit a "flattening" at higher densities, with the onset point increasing with P_{heat}. Fig. 1c demonstrates the almost linear relationship between P_{down} and I_{sat} whereby this connection remains intact even for a density ramp. Fig. 2 considers a 2nd set of discharges, now as density ramps to higher $\bar{n}_e$ values (0.15-1.1x10^{20} m^{-3}), with P_{ecrh} = 0.5, 1, 1.5MW and with the same magnetic field configuration as the HIDC discharges discussed below. A "flattening" of P_{down} with n_{es} and increase with P_{ecrh} is also extant.

2.2 Improved High-Density Confinement: The advent of divertor operation has opened the door to a new high-density operational regime, whereby energy confinement τ_E continues to increase with $\bar{n}_e$ up to ~2x10^{20} m^{-3} and at the same time particle confinement (Al-ablation decay time) decreases (Fig. 3a)/1/. Quasi steady-state discharges - characterized by high

radiation levels concentrated at the edge (P_{rad}/P_{abs} up to ~90%, Fig. 3b), with little impairment of core energy can be reproducibly established. Further, in contrast to "normal" discharges, the density profiles become broader with $\bar{n}_e$ (for $\bar{n}_e<2x10^{20}$ m^{-3}), yielding $n_{es}\sim \bar{n}_e^{1.6\text{-}1.9}$, for P_{nbi}~1-2MW respectively (Fig. 3c, d)...and enabling partial plasma detachment at the target plates for adequate $\bar{n}_e$. Interestingly, above $\bar{n}_e\sim2x10^{20}$ m^{-3}, n_{es} remains constant around $6x10^{19}$ m^{-3} (for P_{nbi}=2MW) up to the onset of detachment at $\bar{n}_e\sim3.2x10^{20}$ m^{-3}.

Fig. 4 exhibits the temporal development of a discharge first established in an attached state and then driven via a gas puff into a strongly partially-detached condition. Here, n_{es} (Fig. 4b) decreases in the latter phase, along with W_{dia}. Accompanying the high P_{rad}/P_{abs} level (~90%) is a dramatic increase in P_{up}, while P_{down} falls slightly (Fig. 4c, 3g). This asymmetry between P_{up} and P_{down} is correlated with P_{rad}/P_{abs} (Fig. 5). Otherwise, the weakly-detached cases (for 1MW: $\bar{n}_e>2.2x10^{20}$ m^{-3}) are attained with moderate gas puff rates and lower P_{rad}/P_{abs}.

The sum of I_{sat} to all target plate Langmuir probes (36 per target, fig. 3e) shows no saturation with n_{es} over a wide n_e range, in contrast to the case of "normal" discharges. The subdivertor pressure follows $P_{div}\sim I_{sat}^{1.4}$ (the averaged pressure P_{div} is given in fig. 3f), but at detachment P_{div} decouples from I_{sat} - remaining either constant or increasing dramatically, depending on P_{rad}/P_{abs}. Finally, the ratio P_{side}/P_{div} (fig.3h), a measure of neutral decompression, exhibits a continual increase with $\bar{n}_e$, becoming particularly large for weak detachment.

3. Discussion: For the case of "normal " confinement, i.e. increase of both τ_E and τ_p with density (for nbi and ecrh), past experience was a concurrent peaking of the density profiles - making it difficult to attain edge densities compatible with good divertor operation. This phenomenon continues to be observed, but now with the unexpected result that particle fluxes to the target plates increase less than linearly with upstream density n_{es} and even "flatten". Such behavior appears to be consistent with the assumption of perpendicular particle transport D_p varying as $1/n_{es}$...demonstrated by modeling two discharges with n_{es} ~1 & $2x10^{19}$ m^{-3} using the edge transport code EMC3-EIRENE /5/. The same calculations predict a similar behavior of pressure, correctly giving the trend and even the absolute P_{div} values within ~30%. In like fashion, the increase in I_{sat} and P_{down} with power might be interpreted as an increase in D_p which is seen in the core plasma and documented in the SOL for other configurations.

With respect to the relationship of $n_{es}/\bar{n}_e$, the two "normal" datasets (D^+, H^+, slightly different configurations) display the same trends but different absolute values. This is at least partly due to the methods used to pinpoint the separatrix position R_s. For the steady-state set, for want of other information, that spatial point on the Li-beam delivering twice the peak target plate density was defined as being R_s. Modeling indicates the ratio will be less, meaning n_{es} is actually smaller. Here this correction has not been implemented, as the main point is to manifest tendencies. For discharges with the second configuration (normal 2, IHDC), the two-point model was used to estimate the upstream temperature necessary to drive the power flux to the target plate (attached cases). This point was located within the T_e-profiles delineated by the edge Thomson-scattering system and the corresponding density noted, thereby defining the separatrix position on the Li-beam. Absolute errors of 20-30% in n_{es} are possible. Nonetheless, relative trends are not affected, which evince a low degree of scatter.

The IHDC regime is accompanied by higher $n_{es}/\bar{n}_e$, facilitating detachment. More studies are needed to clarify why n_{es} ceases to increase with $\bar{n}_e$ beyond a certain limit. Nevertheless, I_{sat} and P_{div} augment continuously with n_{es} (not shown: $I_{sat}\sim n_{es}^{0.66}$ up to the rollover, $P_{div}\sim n_{es}$ up to detachment) - whereby the target plate densities are always < n_{es}. In other words, detachment is realized without passing through a high-recycling regime in strong contrast to tokamaks, and qualitatively consistent with EMC3-EIRENE predictions. The asymmetry between P_{down}

and P_{up} with larger P_{rad}/P_{abs} is not understood. The fact that P_{div} does not fall off at detachment (since P_{down} decreases and P_{up} increases) may have to do with the fact that one small zone on the target plates remains attached (T_{ed}~30ev, otherwise <10eV) in spite of rather advanced detachment elsewhere /1/.

4. Conclusions: The average subdivertor pressure $P_{div}=(P_{up}+P_{down})/2$ varies either ~ linearly with I_{sat} (normal) or as ~ $I_{sat}^{1.4}$ (IHDC), except near/at detachment. For IHDC, P_{div} is roughly proportional to n_{es} over the entire range. However, strong P_{down}- P_{up} asymmetries develop with increasing P_{rad}/P_{abs} - becoming particularly large at detachment where P_{down}/P_{up}~0.26 can prevail, with P_{up} ~4×10^{-3} mbar. Otherwise, P_{div} ~$1\text{-}1.5\times10^{-3}$ mbar for $\bar{n}_e>2\times10^{20}$ m^{-3} and n_{es}~ $4\text{-}6\times10^{19}$ m^{-3}. For orientation, EIRENE calculations predict that P_{div} ~4×10^{-4} mbar is necessary to pump the particle flux associated with P_{nbi}=2MW, assuming a 2% molecular sticking coefficient in the Ti-gettering areas of the subdivertor. Gettering has yet to be activated.

Neutral compression P_{div}/P_{side} becomes poorer with increasing $\bar{n}_e$, varying over ~20-10 up to detachment, and then assuming values as low as five for weak detachment. Apparently, for the open divertor configuration and the low-recycling plasma at the target plates, plasma plugging is not effective in retaining neutrals within the divertor region.

For "normal" cases, EMC3-EIRENE calculations indicate the less-than-linear increase of I_{sat} and P_{div} with n_{es} can be attributed to a decline of perpendicular particle transport in the SOL with increasing $\bar{n}_e$. This trend is not seen with IHDC, where at least the core plasma shows a decrease of τ_p with $\bar{n}_e$. A possible corollary of such τ_p -behavior is the usual peaking of the core density profile (n_{es}~$\bar{n}_e^{0.6}$) vs. the broadening for IHDC (n_{es} ~$\bar{n}_e^{1.6\text{-}1.9}$, 1-2MW).

References:

1) P.Grigull, K.McCormick et al., invited talk, this conference
2) H.Ehmler et al., this conference
3) K.McCormick et al., J. Plasma Phys. Controlled Fusion **41** (1999) B285
4) K.McCormick et al., J.Nucl. Mater. **290-293** (2001) 920
5) F.Gadelmeier et al., this conference

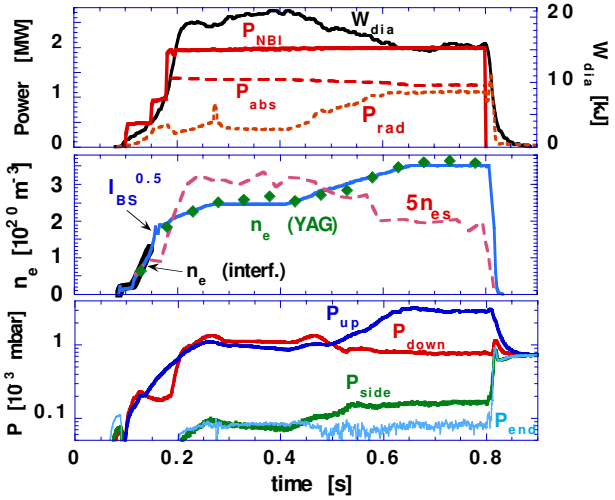

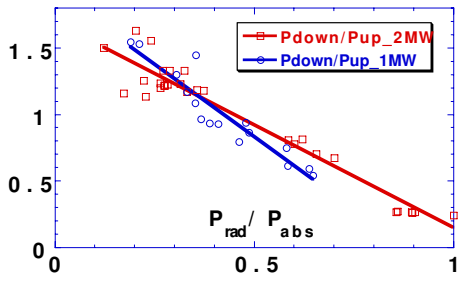

Fig. 5: (above) P_{down}/P_{up} vs. P_{rad}/P_{abs} P_{rad}/P_{abs} =total radiated power, measured in a poloidal plane outside the divertor, normalized to the absorbed NBI power.

Fig. 4: (a-b-c top to bottom) Temporal behavior of core- and edge-parameters for #51321, first established under attached target plasma conditions and driven by gas puffing into a strongly-detached state (over most of the target plate area). W_{dia} = diamagnetic energy; P_{abs} = absorbed power; $I_{BS}^{0.5}$ = Bremsstrahlung signal, indicative of $\bar{n}_e$, used to feedback control the density since $\bar{n}_e$ is too high for the interferometers; n_e(YAG)= $\bar{n}_e$ from Thomson scattering. P_{xx} = neutral pressures in up-down subdivertors and main chamber. ι_a~5/9, H^o -> H^+ , B_t = 2.5T .

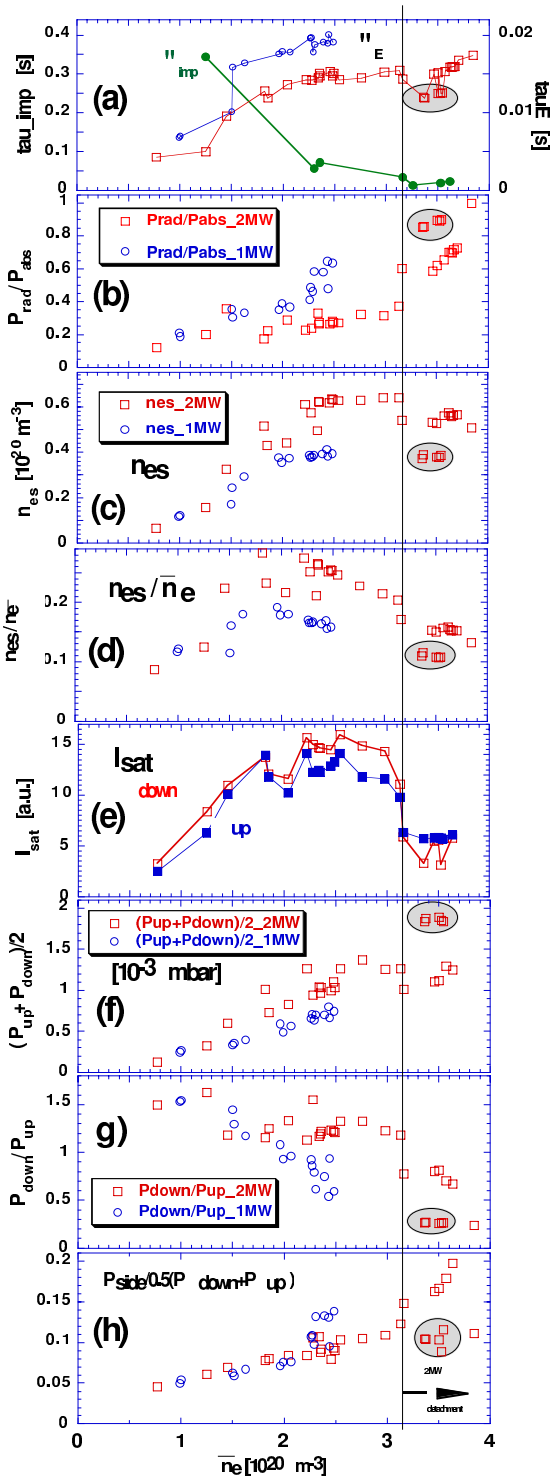

Fig. 3: Database for IHDC quasi steady-state discharges. $\bar{n}_e$ is used as the ordering parameter. Onset of 2MW detachment is marked by the vertical line. Shaded regions delineate strong detachment. P_{nbi}=1, 2MW: H^o->H^+.

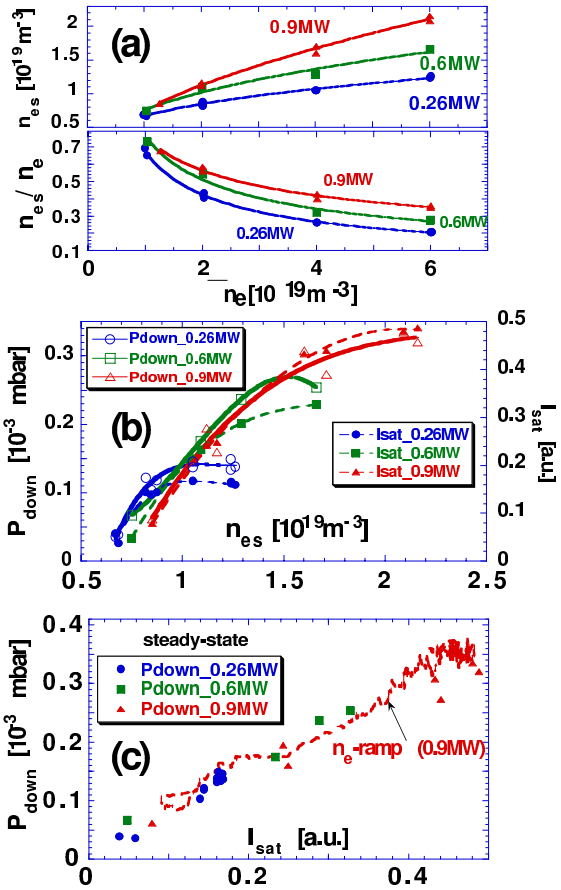

Fig. 1: (a) n_{es} & n_{es}/n_e vs. $\bar{n}_e$; (b) P_{down} & I_{sat} vs. n_{es}; (c) P_{down} vs. I_{sat} for quasi steady-state database and n_e-ramp. "Normal confinement". P_{ecrh}=0.3, 0.6 & 0.9MW. D^+, B_t=2.5T.

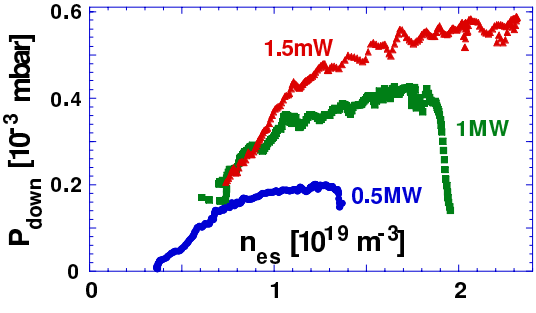

Fig. 2: P_{down} vs. n_{es} for the configuration of fig.3. "Normal confinement". Density ramps over $\bar{n}_e$ ~ 0.15 - 1.1x10^{20} m^{-3}. P_{ecrh} = 0.5, 1, 1.5MW. H^+, B_t = 2.5T .